Addressing Nonlinear Relative Motion For Spacecraft Collision Probability

Salvatore Alfano*
Center for Space Standards and Innovation, Colorado Springs, Colorado, 80132

Linear methods for computing satellite collision probability can be extended to accommodate nonlinear relative motion in the presence of changing position and velocity uncertainties. Collision probability analysis for spherical objects exhibiting linear relative motion is accomplished by combining covariances and physical object dimensions at the point of closest approach. The resulting covariance ellipsoid and hardbody are projected onto the plane perpendicular to relative velocity by assuming linear relative motion and constant positional uncertainty throughout the brief encounter. Collision potential is determined from the object footprint on the projected, two-dimensional, covariance ellipse. For nonlinear motion, the dimension associated with relative velocity must be reintroduced. This can be simply done by breaking the collision tube into sufficiently small cylinders such that the sectional motion is nearly linear, computing the linear probability associated with each section, and then summing. The method begins with object position and velocity data at the time of closest approach. Propagation of position, velocity, and covariance is done forward/backward in time until a user limit is reached. An alternate method is presented that creates a voxel grid in Mahalanobis space, computes the probability of each affected voxel as the combined object passes through the space, and sums. These general methods are not dependent on a specific propagator or linear probability model.

Nomenclature

erf	=	error function
M_f	=	final Mahalanobis distance
M_i	=	initial Mahalanobis distance
n	=	covariance ellipsoid scale factor
p	=	probability
P_{1d}	=	one-dimensional probability
R	=	radius of torus
r	=	cross-sectional radius
x	=	integration variable
σ	=	standard deviation

* Technical Program Manager, CSSI, 7150 Campus Drive, Suite 260, Colorado Springs, CO, 80920-6522, salfano@centerforspace.com, AIAA Associate Fellow.

I. Introduction

The assumptions involved in linear collision probability formulation are well defined in References 1-4 and are summarized here for the reader's convenience. Space object collision probability analysis (COLA) is typically conducted with the objects modeled as spheres, thus eliminating the need for attitude information. Their relative motion is considered linear for the encounter by assuming the effect of relative acceleration is dwarfed by that of the velocity. The positional errors are assumed to be zero-mean, Gaussian, uncorrelated, and constant for the encounter. The relative velocity at the point of closest approach is deemed sufficiently large to ensure a brief encounter time and static covariance. The encounter region is defined when one object is within a standard deviation (σ) combined covariance ellipsoid shell scaled by a factor of n. This user-defined, three-dimensional, n-σ shell is centered on the primary object; n is typically in the range of 3 to 8 to accommodate conjunction possibilities ranging from 97.070911% to 99.999999%.

Because the covariances are expected to be uncorrelated, they are simply summed to form one, large, combined, covariance ellipsoid that is centered at the primary object. The secondary object passes quickly through this ellipsoid creating a tube-shaped path that is commonly called a collision tube. A conjunction occurs if the secondary sphere touches the primary sphere, i.e. when the distance between the two projected object centers is less than the sum of their radii. The radius of this collision tube accommodates all possibilities of the secondary touching the primary by combining the radii of both objects. A plane perpendicular to the relative velocity vector is formed and the combined object and covariance ellipsoid are projected onto this encounter plane.

As previously stated, the encounter region is defined by an n-σ shell determined by the user to sufficiently account for conjunction possibilities. Within that shell the tube is straight and rapidly traversed, allowing a decoupling of the dimension associated with the tube path (relative velocity). The tube becomes a circle on the projected encounter plane. Likewise, the covariance ellipsoid becomes an ellipse. The relative velocity vector (decoupled dimension) is associated with the time of closest approach. The conjunction assessment here is concerned with cumulative probability over the time it takes to span the n-σ shell, not an instantaneous probability at a specific time within the shell. Along this decoupled dimension, integration of the probability density across the shell produces a number very near unity, meaning the close approach will occur at some time within the shell with near absolute certainty. Thus the cumulative collision probability is reduced to a two-dimensional problem in the encounter plane that is then multiplied by the decoupled dimension's probability. By rounding the latter probability to one, it is eliminated from further calculations. Thus the projection results in a double integral that can be reduced to a single integral by using the error function or a contour integral.

The assumption of linear relative motion may not be valid in all cases. Chan[5] proposed test criteria for nonlinearity. Both Chan[5] and Patera[6] published different methods for calculating collision probability for such instances. Nonlinear motion is typically associated with long-term encounters which imply the covariance can no longer be assumed static. The collision tube will not be straight, invalidating the simple dimensional reduction used for linear motion. The size of the n-σ shell must also be carefully considered, especially if the relative motion reverses direction during the encounter.

Two methods are presented in this paper. The first method adjoins tubes in Cartesian space, eliminating the conversion to Patera's symmetrized space and subsequent object distortion. Probability computations for spherical[4] and rectangular[7] objects are then assessed and compared to existing published cases. The second method creates a voxel grid in Mahalanobis space and is more computationally intense than the first method. The probability of each affected voxel is computed as the combined object passes through the space, then all are summed. These general methods are not dependent on a specific propagator or linear probability model. Practical considerations are addressed for both.

II. Adjoining Tubes

Linear methods for computing satellite collision probability can be extended to accommodate nonlinear relative motion in the presence of changing position and velocity uncertainties. For linear relative motion, the probability along the relative velocity vector (collision tube) is unity and is conveniently removed from the calculations. For nonlinear motion, that dimension must be reintroduced. This can be simply done by breaking the collision tube into small sections, computing the probability associated with each section, and then summing. To accomplish this, an orbit propagator is needed that can propagate satellite position, velocity, and associated covariances. The propagator must be of sufficient accuracy to meet user requirements. For testing purposes, a simple two-body propagator was used.

A. General Method

The general method of adjoining tubes begins with object position and velocity data at the time of closest approach. Propagation is done forward/backward in time until a user limit is reached. The limit can be based on a standard deviation threshold (3σ was recommended by Patera[6]) or a specified time (such as one orbital period). For each time step the tube sections should be sufficiently small enough so that, over the interval, the relative motion can be assumed linear and the covariance constant. For each section, a two-dimensional probability is computed as previously described for linear motion by projecting the combined object shape onto a plane perpendicular to the relative velocity. In addition, a one-dimensional probability is computed along the relative velocity vector by determining the component position from the mean at each end of the tube and then dividing by the standard deviation for that axis, thus producing each endpoint's Mahalanobis[8] distance. The product of these probabilities yields the sectional probability. All sectional probabilities are summed until the time and/or sigma limit is reached. This approach differs from Patera[6] in that no symmetrized scaling is done. The probability of each cylinder is determined by multiplying the two-dimensional linear probability by the sectional (relative velocity axis) probability; the user may choose any linear probability model[3-7].

The tubes have no gaps when dealing with linear relative motion. For such cases, the nonlinear results will perfectly match the linear probability for constant covariance and objects of any shape. As seen in Figure 1, nonlinear motion causes gaps and overlaps where the tube sections meet. If the relative motion track bends towards the covariance ellipsoid center, then the overlapping sections will occur in regions of greater probability density with the gaps occurring in regions of lesser probability density. Although the gap and overlapping volumes are almost equal, the resulting summation causes an over inflation of the probability. If the relative motion track bends away from the covariance ellipsoid center, then the probability for cylindrical tubes will be underestimated because the gap is in a region of higher probability density. The amount of error will vary based on the degree of bending/overlap relative to probability density. The testing of this method matched all the examples presented by Patera[6], including the stressing torroid example.

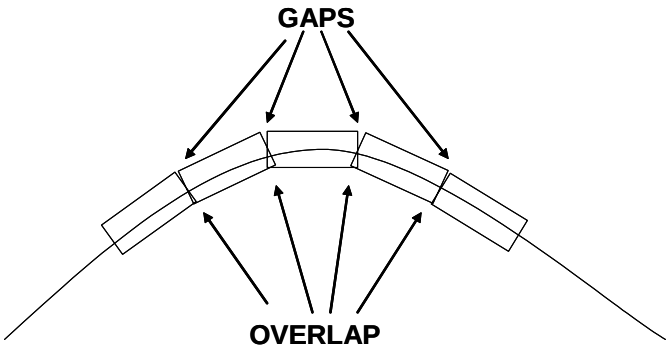

Figure 1. Tube Sections for Nonlinear Relative Motion Track.
Nonlinear motion causes gaps and overlaps where the tube sections meet.

There are several choices the reader should carefully consider when implementing this method. The limits and time step must be selected to ensure adequacy for the intended analysis. For a very large time limit and cyclical relative motion it is possible to retrace the same path through the covariance space. An example would be one satellite circling the other in formation for hundreds of revolutions. The collision tube would continually trace over itself; if care is not taken, the single revolution probability could be summed hundreds of times. To avoid this, it is suggested that the total time limit not exceed one orbital period or that subsequent retracing be recognized and suitable adjustments made to the calculation. A large time step can also cause errors if the sectional motion is not sufficiently linear or the sectional covariance is not sufficiently constant. A simple test for sufficiency is to halve

the time step and repeat the analysis. If the probability differences are within the user's tolerance, then the time step is adequate.

B. Sectional Computation

Three-dimensional position and velocity data of each object, as well as their 6x6 covariance matrices, are required. Although not necessary, this paper assumes all starting data to be at the point of closest approach in the Earth Centered Inertial (ECI) frame. Suitable incremental limits should be set for the time step, maximum acceptable angle between adjoining tubes, and maximum change in long-axis sigma for any tube. Additionally, the user must specify the computational stopping condition in terms of time limit and/or encounter region. Any linear probability model can be chosen for the method that follows.

To compute the sectional probability of each tube, all data is propagated for the given time step. If the angular difference between the previous and current relative velocity vectors exceeds the angular limit, the time step is halved and this process repeated. A coordinate transformation is accomplished to align the z axis with the relative velocity vector. The one-dimensional, z-axis, Mahalanobis[8] distances of the cylinder endpoints (M_i, M_f) are used to compute long-axis probability P_{1d} from

$$P_{1d} = \left| \frac{1}{2} \cdot \left(\operatorname{erf}\left(\frac{M_f}{\sqrt{2}} \right) - \operatorname{erf}\left(\frac{M_i}{\sqrt{2}} \right) \right) \right| \tag{1}$$

If the endpoint differences should exceed the maximum change in long-axis sigma then the time step is halved and this process repeated. Projection of the collision tube onto the encounter plane, defined by the x-y axes, produces the necessary information to generate two-dimensional collision probability using whatever method the user chooses. The one- and two-dimensional probabilities are then multiplied to determine the sectional collision probability. This process is repeated until a final limit is reached.

C. Practical Considerations

The incremental limits chosen for this paper were determined by trial and error to achieve a balance between processing speed and numerical accuracy. The maximum time step was set to 100 seconds, the maximum acceptable angle between adjoining tubes was one degree, and the maximum change in long-axis sigma for any tube was 0.25 σ. At the beginning of each iteration the time step was increased by 25%. If the incremental results exceeded any limit, the time step was halved and the incremental calculations repeated. This prevented small iterative steps required for one part of the trajectory from retarding calculations elsewhere. The time limit was set to one orbital period (half orbit forward and half orbit backward from closest approach point) and the encounter shell's scale factor set to 10 (n=10). Once the overall limit was reached, the entire process was repeated with all incremental limits halved. If the results agreed to within two significant figures, the calculated probability was considered suitable.

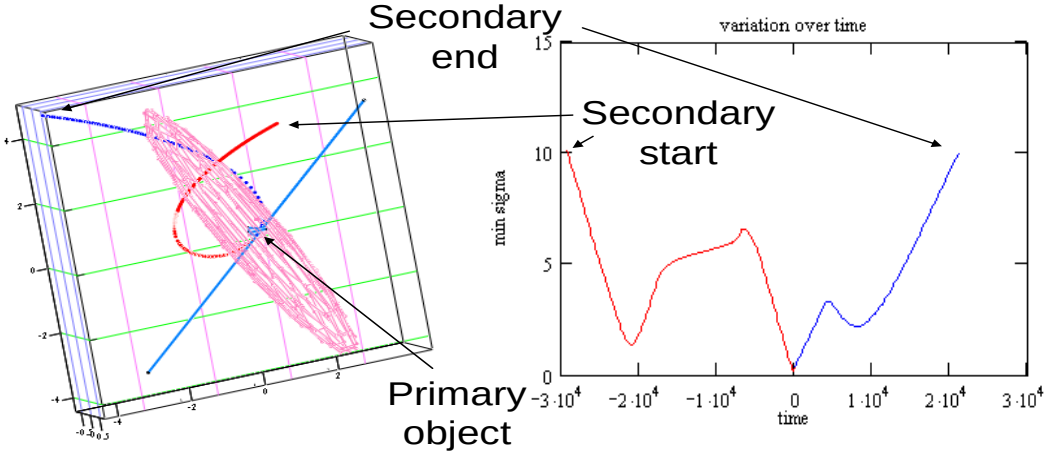

Figure 2. Nonlinear Relative Motion.
Trajectory exits and reenters encounter region depicted by a 3σ ellipsoidal shell.

The 3σ encounter shell suggested by Patera[6] was insufficient for some cases where the relative trajectory reversed itself. Consider the linear and nonlinear motion shown in Figure 2. The nonlinear relative motion is such that the trajectory exits and reenters the 3σ encounter shell both before and after the close approach point. The positional history represented by the Mahalanobis[8] distance is plotted versus time in seconds on the right. With a final calculation limit of 3σ, the nonlinear probability is 0.000747. Expanding the limit to 10σ, the nonlinear probability is 0.00111. In this case, the 3σ limit did not fully capture the encounter. As a point of reference, the linear probability was 0.000469.

The linear maximum probability method[9] was originally designed to rescale and reorient the two-dimensional covariance in the encounter plane through a single-axis rotation. With the re-introduction of the third dimension, reorientation requires a two-axis rotation. The original method should not be applied here because it is not sufficient to address the third dimension. Three-dimensional reorientation to assess maximum probability will be the subject of future work.

D. Numerical testing

Testing was done by comparing the method to linear cases and Patera's nonlinear cases. As expected, the method perfectly matched the linear cases. The convergence behavior for the nonlinear torroidal[6] case differed from Patera's method and presents a good illustration of practical considerations.

A circular, relative trajectory is chosen with a spherical hardbody radius and symmetric covariance ellipsoid. The object creates a torus as it follows the circular trajectory. The exact solution to collision probability was derived by Chan[10] as

$$p = \frac{2}{\sigma}\cdot\sqrt{\frac{2}{\pi}}\cdot\exp\left[\frac{-\left(R^2+r^2\right)}{2\cdot\sigma^2}\right]\cdot\int_0^r \sinh\left(\frac{R\cdot\sqrt{r^2-x^2}}{\sigma^2}\right)dx \tag{1}$$

where σ is the standard deviation, R is the radius of the torus, and r is the cross-sectional radius as shown in the following figure.

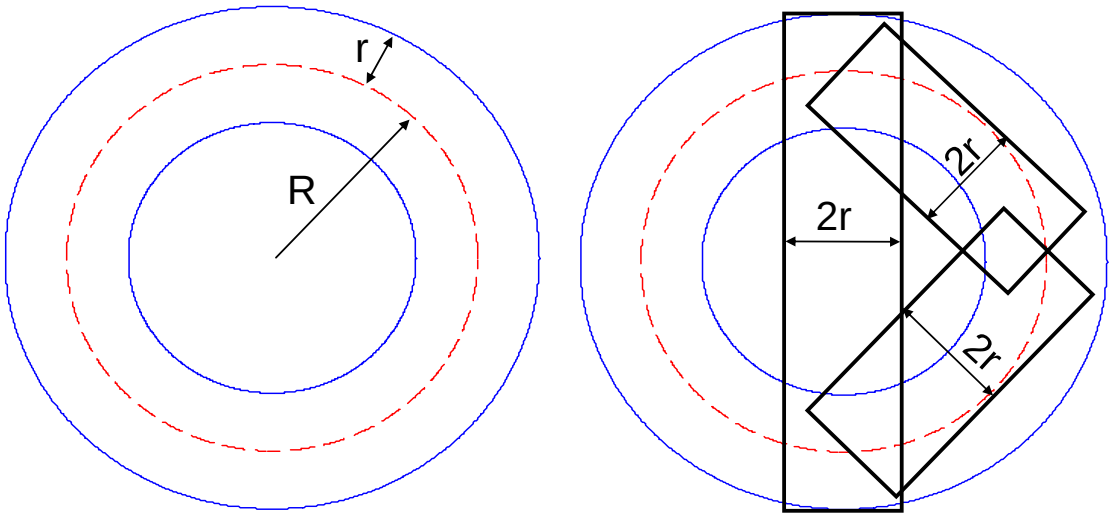

Figure 3. Circular Relative Motion Test Case.
Torus depiction and under-represented cylindrical representations.

The collision tube is more closely represented as the number of cylinders increases. With σ set to one, R set to one, and r set to 0.3, Eq. 1 produces a probability of 0.066144. The number of adjoining cylinders was varied from 4 to 300 to assess convergence behavior as displayed in Figure 4.

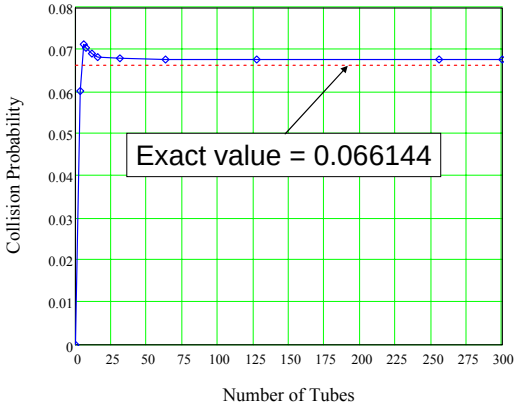

Figure 4. Convergence behavior for torroid test case.

Representing the torrus with 300 adjoining cylinders, the probability value was 0.06765. This is an overestimate of 2.3% and is in agreement with Patera. Because the tube bends towards the origin, the cylinders will overlap in regions of greater probability density and cause an overestimation. In the cases where few cylinders are used, this method tended to overestimate while Patera's consistently underestimated. The collision probability calculation does not require a large number of tubes. Even with an angle limit of 5 degrees, the probability is 0.06767, suggesting that the test for nonlinearity given by Chan[5] may be relaxed in certain cases.

Patera's other test cases were modeled and matched with the exception of the geosynchronous example due to insufficient data. Testing of rectangular objects was also accomplished and all linear cases were matched. Nonlinear cases produced intuitive results with probability decreasing with width factor, but there is nothing published with which to compare.

III. Voxels

The following method uses volume elements (voxels[11]) for computing satellite collision probability and does not employ other probability methods. The collision tube is propagated and transformed to Mahalanobis[8] space using the time-varying covariance. The Mahalanobis space is partitioned using voxels. The probability of each voxel touched by the tube is computed and all are summed to produce the overall collision risk.

A. General Method

As in the former section, the method of voxels begins with object position and velocity data at the time of closest approach. Propagation is done forward/backward in time until a user limit is reached as previously described. At every time step, the objects and their positional covariances are transformed to the Mahalanobis space by converting their Cartesian distances to Mahalanobis distances. An assessment is made to determine what voxels are contained within the combined, transformed hardbody. If any of those voxels were contained in previous iterations, they are eliminated from further consideration. The probabilities of the remaining voxels are computed and added to the running probability total.

B. Incremental Computation

Three-dimensional position and velocity data of each object, as well as their 6x6 covariance matrices, are required. Again the assumption is made that all starting data are at the point of closest approach in the Earth Centered Inertial (ECI) frame. Suitable incremental limits should be set for each time step so that no voxels are skipped as the combined object passes through the Mahalanobis space. As in the previous method, the user must specify the computational stopping condition in terms of time limit and/or encounter region. Additionally, it is recommended that for each time step all data be converted to a suitable frame that rotates with the orbit. For this paper the Velocity-Normal-Co-Normal (VNC) frame was used.

The Mahalanobis space has unit variance along each dimension. The transformation begins by determining the eigenvalues and associated eigenvectors of the combined covariance matrix. The eigenvectors are used to reorient all data while diagonalizing the covariance. All data is then scaled using the corresponding eigenvalues so that the covariance matrix becomes the identity matrix. Reverse reorientation is done and a determination made as to which voxels are contained in the combined object hardbody.

C. Practical Considerations

The reverse reorientation mentioned previously is done to eliminate the need to associate the covariance ellipsoid axes from one time step to the next. As the covariance changes shape and orientation over time, it is possible that a minor axis in a previous iteration becomes a major axis in the next. It is not uncommon for eigenvalue solving routines to order their outputs from least to greatest or vice-versa. Without associating the axes from step to step, the corresponding eigenvalues could reorder the axes, thereby causing a sudden axis swap which would appear as an abrupt 90^0 reorientation in the transformed space. By using the same ordered eigenvectors to reverse the reorientation, any axis swap that might occur is undone.

Another consideration is the frame choice. As seen in the Figure 5, relative motion can appear quite different in different frames. Consider the case of a time-invariant, combined covariance that is represented by the identity matrix with a secondary object 1.5 kilometers ahead of the primary in otherwise identical circular orbits. In the

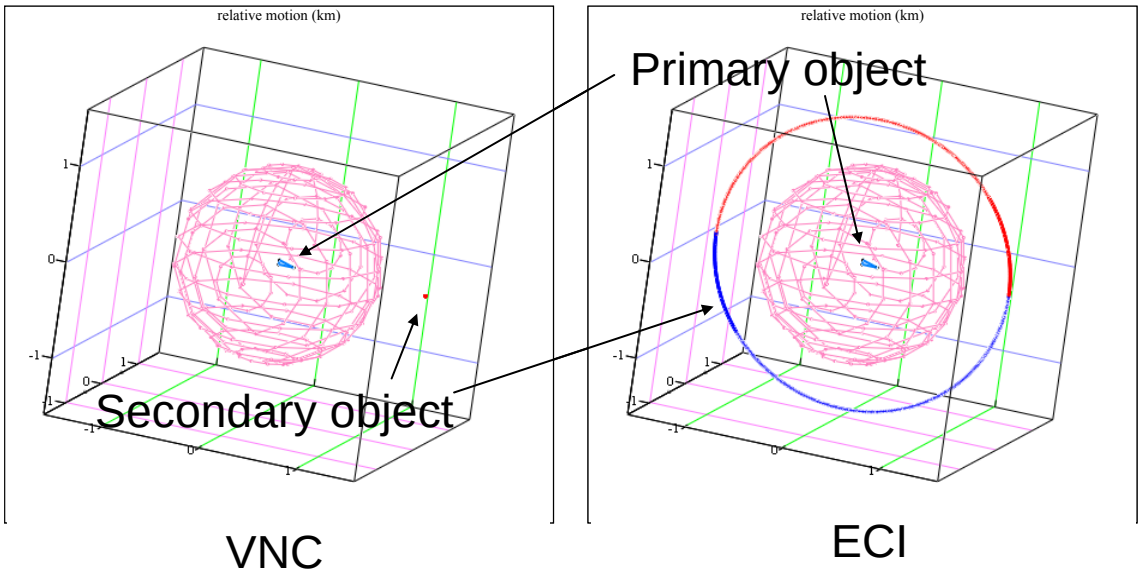

Figure 5. Apparent Relative Motion in Mahalanobis Space
Trajectory path in VNC and ECI frames about a 1σ ellipsoidal shell.

VNC frame, the secondary object would appear as a static sphere. In Mahalanobis space the combined hardbody would also appear as a static sphere and affect very few voxels. In the ECI frame, the secondary would appear to circle the primary in the course of a single orbit and, on initial inspection, affect many voxels along this path. To accommodate the latter case, the voxel grid in Mahalanobis space should be rotated with the orbit. For this work, the VNC frame was chosen to simplify computations.

Due to time correlation, apparent motion in Cartesian space can be misleading when working in Mahalanobis space. Again consider the case of a secondary object 1.5 kilometers ahead of the primary in otherwise identical circular orbits, but with a growing covariance as depicted in Figure 6. In Cartesian space the secondary object would appear fixed in relative space as the covariance ellipsoid grows with time and envelops it. In Mahalanobis space the secondary would appear to move towards the primary and affect many more voxels along this path. To address this time correlation, all probability calculations are done in the Mahalanobis space.

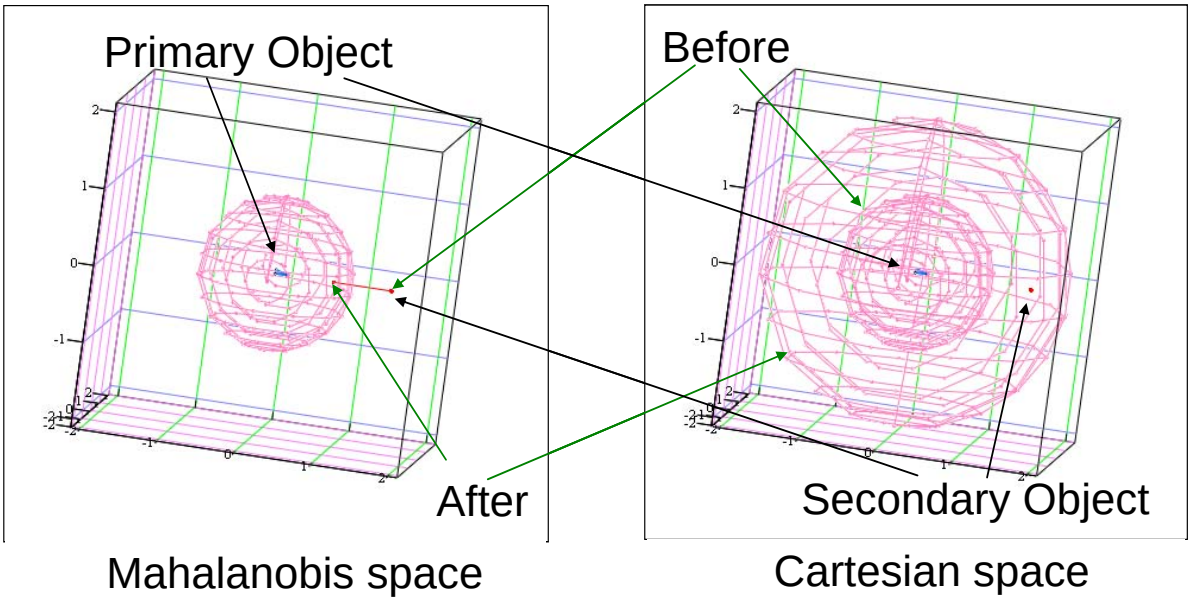

Figure 6. Apparent Relative Motion in Different Spaces
Trajectory behavior in Mahalanobis and Cartesian space, respectively.

Obviously, if the number of divisions per sigma are small, the voxels will be large and encompass more volume than the hardbody. As the divisions increase so does fidelity, with the voxels becoming more representative of the combined object's shape as seen in Figure 7. For the torus, the upper-right voxels depicted by red squares outlined with heavy black lines overestimate the object. The lower-left voxels depicted with green outlines more closely estimate the object.

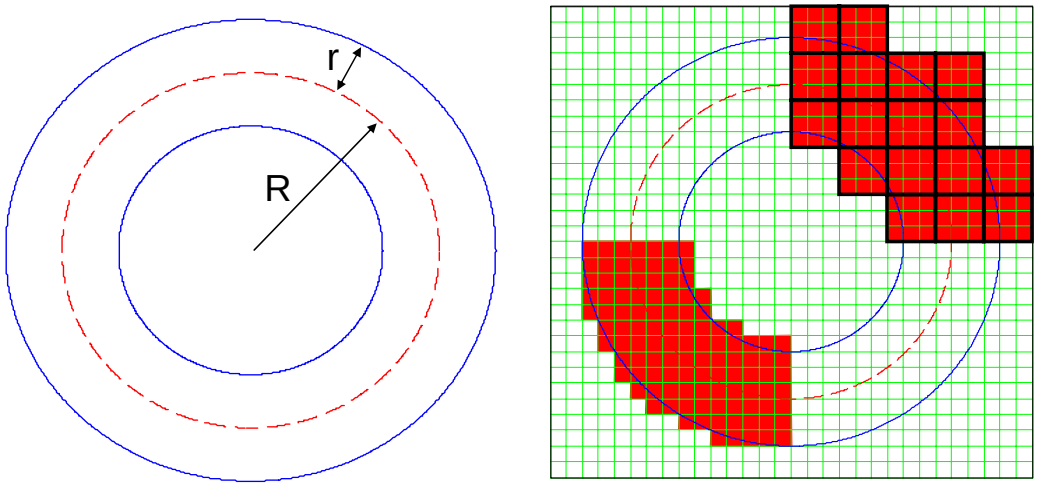

Figure 7. Voxel size affects object representation
Torus depiction and over-represented voxel representations.

Spherical objects can be severely distorted when transformed to the Mahalanobis space. The same transformation that makes an elongated covariance ellipsoid a unit sphere will cause a spherical hardbody to become an ellipsoid. The user should choose a voxel size that is sufficiently small to properly represent the object. One approach is to repeat the computations with half the voxel size. If the results agree to within two significant figures, the voxel size and associated probability are considered suitable. If not, then halve the voxel size again and repeat the process. Figure 8 shows the behavior for a torroid test case.

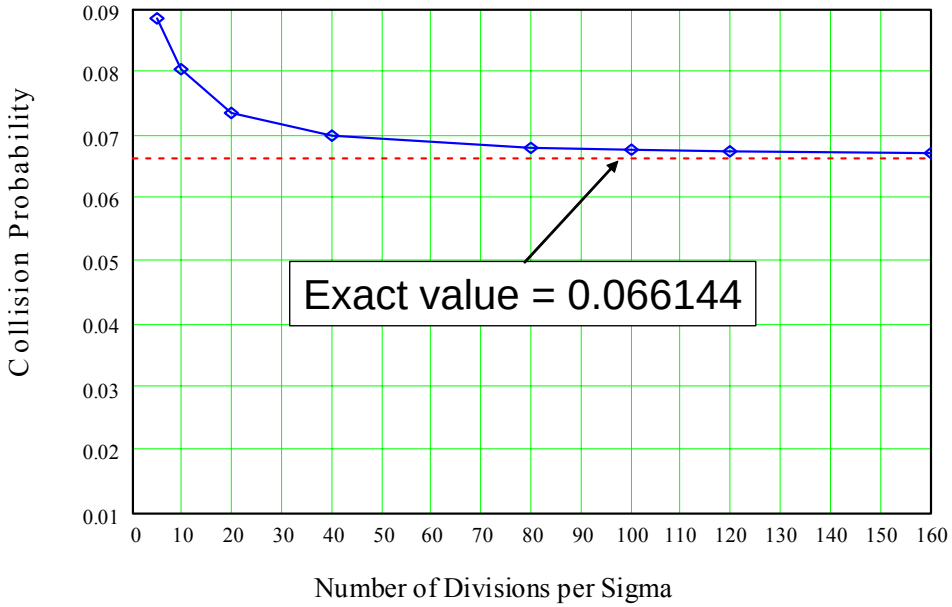

Figure 8. Convergence behavior for torroid test case using voxels

D. Numerical testing

As with the adjoining cylinders, testing was done by comparing the method to linear cases and Patera's nonlinear cases. As expected, the method closely matched those cases. For rectangular objects with nonlinear motion, no test cases exist with which to compare.

In testing, this voxel method consumed much memory and processing time. This was partially addressed by limiting the number of voxels previously touched (fading memory) and using a sliver of the projected object that was three voxels thick rather than the complete sphere or rectangle. Results were nearly identical to the full method, but still quite time consuming. Even with these refinements, computations with a 3 gigahertz processor often ran slower than real time. With current memory and processing speed, this method is best suited for test case generation.

IV. Conclusion

Two methods were presented for determining collision probability in the presence of nonlinear relative motion. Both methods produced acceptable results with previously published test cases. The methods also incorporate dynamic covariance although no test cases could be found in the public literature with which to compare.

The first method extends linear methods by representing the collision tube as a series of adjoining tubes in Cartesian space. The probability associated with the changing relative velocity direction is addressed because the collision tube is not straight, invalidating the simple dimensional reduction used for linear motion. Incremental limits of 100 seconds for maximum time step, one degree for maximum acceptable angle between adjoining tubes, and 0.25 σ for the maximum change in long-axis sigma for any tube were sufficient to achieve at least two significant figures of accuracy when calculating probability.

The second method represents the collision tube as voxels in Mahalanobis space. It was shown that apparent motion in Cartesian space can be misleading when working in Mahalanobis space. Also, the covariance ellipsoid becomes a unit sphere that maintains its size and shape regardless of rotation; the voxel grid in Mahalanobis space, however, must be rotated with the orbit. The voxel size must be carefully selected to ensure the object is not over-represented. Based on current computer memory and processing speed, this method is recommended only for determining reference cases.

References

[1]Alfriend, K. T., Akella, M. R., Frisbee, J., Foster, J. L., Lee, D. J., and Wilkins, M. "Probability of Collision Error Analysis," *Space Debris*, Vol. 1, No. 1, 1999.

[2]Akella, M. R. and Alfriend, K. T., "Probability of Collision Between Space Objects," *Journal of Guidance, Control, and Dynamics*, Vol. 23, No. 5, September-October 2000, pp. 769-772.

[3]Patera, R. P. "General Method for Calculating Satellite Collision Probability," *Journal of Guidance, Control, and Dynamics*, Vol. 24, No. 4, July-August 2001, pp. 716-722.

[4]Alfano, S. "A Numerical Implementation of Spherical Object Collision Probability," *Journal of the Astronautical Sciences*, Vol. 53, No. 1, January-March 2005, pp. 103-109.

[5]Chan, K., "Short-Term vs Long-Term Spacecraft Encounters," AIAA Paper No. 2004-5460, AIAA/AAS Astrodynamics Specialist Conference, Providence, Rhode Island, 16-19 August, 2004.

[6]Patera, R. P., "Satellite Collision Probability for Nonlinear Relative Motion," *Journal of Guidance, Control, and Dynamics*, Vol. 26, No. 5, September-October 2003, pp. 728-733.

[7]Alfano, S. " Satellite Collision Probability Enhancements," *Journal of Guidance, Control, and Dynamics*, Vol. 29, No. 3, May-June 2006, pp. 588-592.

[8]Wikipedia., "Mahalanobis distance," URL: http://en.wikipedia.org/wiki/Mahalanobis_distance [cited 2 June 1998].

[9]Alfano, S. "Relating Position Uncertainty to Maximum Conjunction Probability," *Journal of the Astronautical Sciences*, Vol. 53, No. 2, April-June 2005, pp. 193-205.

[10]Chan, K., "Spacecraft Collision Probability for Long-Term Encounters," AAS Paper No. 03-549, AAS/AIAA Astrodynamics Specialist Conference, Big Sky, Montana, 3-7 August, 2003.

[11]Wikipedia., "Voxel," URL: http://en.wikipedia.org/wiki/Voxel [cited 16 June 1998].